CTGF antagonism with mAb FG-3019 enhances chemotherapy response without increasing drug delivery in murine ductal pancreas cancer

Albrecht Neesse[a,b], Kristopher K. Frese[a], Tashinga E. Bapiro[a,c], Tomoaki Nakagawa[a], Mark D. Sternlicht[d], Todd W. Seeley[d], Christian Pilarsky[e], Duncan I. Jodrell[a,c], Suzanne M. Spong[d], and David A. Tuveson[a,f,1]

[a]Cancer Research UK Cambridge Institute, University of Cambridge, Cambridge CB2 0RE, United Kingdom; [b]Department of Gastroenterology, Endocrinology, and Metabolism, Philipps University Marburg, 35043 Marburg, Germany; [c]Department of Oncology, University of Cambridge, Addenbrooke's Hospital, Cambridge CB2 0QQ, United Kingdom; [d]FibroGen, Inc., San Francisco, CA 94158; [e]Department of General, Thoracic, and Vascular Surgery, University Hospital Carl Gustav Carus, Technical University Dresden, 01307 Dresden, Germany; and [f]Cold Spring Harbor Laboratory, Cold Spring Harbor, NY 11724

Edited by Douglas Hanahan, University of California, San Francisco, CA, and approved June 6, 2013 (received for review January 9, 2013)

Pancreatic ductal adenocarcinoma (PDA) is characterized by abundant desmoplasia and poor tissue perfusion. These features are proposed to limit the access of therapies to neoplastic cells and blunt treatment efficacy. Indeed, several agents that target the PDA tumor microenvironment promote concomitant chemotherapy delivery and increased antineoplastic response in murine models of PDA. Prior studies could not determine whether chemotherapy delivery or microenvironment modulation per se were the dominant features in treatment response, and such information could guide the optimal translation of these preclinical findings to patients. To distinguish between these possibilities, we used a chemical inhibitor of cytidine deaminase to stabilize and thereby artificially elevate gemcitabine levels in murine PDA tumors without disrupting the tumor microenvironment. Additionally, we used the FG-3019 monoclonal antibody (mAb) that is directed against the pleiotropic matricellular signaling protein connective tissue growth factor (CTGF/CCN2). Inhibition of cytidine deaminase raised the levels of activated gemcitabine within PDA tumors without stimulating neoplastic cell killing or decreasing the growth of tumors, whereas FG-3019 increased PDA cell killing and led to a dramatic tumor response without altering gemcitabine delivery. The response to FG-3019 correlated with the decreased expression of a previously described promoter of PDA chemotherapy resistance, the X-linked inhibitor of apoptosis protein. Therefore, alterations in survival cues following targeting of tumor microenvironmental factors may play an important role in treatment responses in animal models, and by extension in PDA patients.

chemoresistance | pancreatic tumor stroma | genetically engineered mouse models

Pancreatic ductal adenocarcinoma (PDA) remains a uniformly lethal disease with a catastrophic 5-y survival rate of less than 5% (1). Despite intensive preclinical and clinical research efforts to tackle this disastrous disease, the oncologic management of PDA patients has hardly changed over the last several decades. The poor responsiveness to standard single and combination chemotherapies is reflected in a median survival of 6–11 mo in advanced disease, and emphasizes the desperate need for novel therapies (2, 3). A striking histological feature of PDA is the extremely dense and highly abundant tumor stroma consisting of activated cancer-associated fibroblasts (CAFs), infiltrating immune cells, and perturbed vascular cells that form a reactive, inflammatory, immunosuppressive, and highly dynamic tumor microenvironment around neoplastic ductal cells. More than in any other solid malignancy, this microenvironmental network of soluble cytokines, growth factors, proteases, and additional extracellular matrix (ECM) components has increasingly been appreciated to support cancer cell proliferation, differentiation, invasion, early metastasis, and therapeutic resistance in PDA (4–7). In contrast to traditional preclinical assays, genetically engineered mouse models (GEMMs) constitute relatively novel tools in preclinical therapeutic testing that elegantly recapitulate the tumor microenvironment in appropriate tissue compartments, thus allowing the evaluation of therapeutic efficacy more accurately (8–10). For pancreatic cancer, the *LSL-Kras$^{G12D/+}$; LSL-Trp53$^{R172H/+}$;Pdx-1-Cre* (KPC) mouse model was generated with conditional mutations in both the *Kras* oncogene and the *p53* tumor-suppressor gene analogous to the genetic mutations found in PDA patients, and may represent a more predictive model for preclinical evaluation compared with historical xenograft models. KPC mice develop endogenous pancreatic adenocarcinomas with 100% penetrance and closely mimic many features of human PDA including extensive desmoplasia, occurrence and site of metastases, cachexia, and ascites formation (11).

We previously established a preclinical therapeutics platform using GEMMs and demonstrated that the pronounced desmoplastic reaction in PDA confers an obstacle to sufficient drug delivery. The combination of Sonic Hedgehog (SHH) inhibition by the semisynthetic cyclopamine derivative IPI-926 and gemcitabine resulted in stromal depletion, significantly increased microvessel density and patency, and improved drug delivery in a GEMM of pancreas cancer (12). In addition, megadalton glycosaminoglycan hyaluronan (HA) is profusely found in the ECM of murine and human PDA and maintains a high interstitial fluid pressure, thus compressing blood vessels (13–15). We and others have recently provided evidence that enzymatic degradation of HA by PEGPH20 significantly increased vessel patency and perfusion without increasing the density of tumor vessels, resulting in increased active gemcitabine levels in the tumor (15, 16). Both the antismoothened and hyaluronidase therapeutic approaches resulted in transient antitumor responses and prolonged survival in the KPC mouse model. However, the aforementioned studies could not address whether the disruption of stromally derived factors also sensitized cancer cells to gemcitabine. Indeed, we also recently published that γ-secretase inhibition synergized with gemcitabine in the same mouse PDA model by cotargeting tumor endothelial cells and neoplastic

Author contributions: A.N. and D.A.T. designed research; A.N., K.K.F., T.E.B., T.N., M.D.S., and C.P. performed research; T.W.S., D.I.J., and S.M.S. contributed new reagents/analytic tools; A.N., K.K.F., M.D.S., T.W.S., C.P., D.I.J., S.M.S., and D.A.T. analyzed data; and A.N., K.K.F., and D.A.T. wrote the paper.

Conflict of interest statement: M.D.S., T.W.S., and S.M.S. are employees of FibroGen, Inc.

This article is a PNAS Direct Submission.

Freely available online through the PNAS open access option.

Data deposition: The complete array results reported in this paper have been deposited in the Gene Expression Omnibus (GEO) database, www.ncbi.nlm.nih.gov/geo (accession no. GSE46203).

[1]To whom correspondence should be addressed. E-mail: dtuveson@cshl.edu.

This article contains supporting information online at www.pnas.org/lookup/suppl/doi:10.1073/pnas.1300415110/-/DCSupplemental.

CELL BIOLOGY

cells, without increasing chemotherapy delivery (17). Therefore, we asked whether increasing chemotherapy concentrations alone is sufficient to elicit improved response rates, or rather that ECM modulation/degradation sensitizes tumors to the antineoplastic properties of chemotherapy. Accordingly, we investigated the function of connective tissue growth factor (CTGF), a protein known to be important in stromal formation. CTGF is a pleiotropic and cysteine-rich matricellular protein that is abundant in many solid malignancies including pancreas, breast, esophageal, glioblastoma, and hepatocellular carcinoma (18–23). CTGF is expressed in both stromal (23, 24) and neoplastic cells (25, 26) of the pancreas, and participates in a variety of signaling pathways that influence pancreatic stellate cell (PSC)-mediated fibrogenesis in pancreatitis and pancreatic cancer. Upon activation of profibrogenic molecules such as TGF-β, CTGF is synthesized and regulates integrin α5β1-dependent adhesion, migration, and collagen I synthesis in PSCs (27, 28). By using an antibody directed against CTGF, we uncouple drug delivery from stromal depletion in KPC mice and propose that CTGF within the tumor microenvironment mediates resistance to gemcitabine in murine PDA.

Results

Isolated Elevation of Active Gemcitabine Triphosphate Does Not Improve Therapeutic Response in Mouse PDA. We have recently shown that pharmacological inhibition of SHH by IPI-926 and the enzymatic degradation of HA by PEGPH20 improved chemotherapy delivery either through increased mean vessel density and stromal depletion or by reexpansion and endothelial fenestration formation of blood vessels, respectively (12, 16). Here we investigated whether increased accumulation of active gemcitabine triphosphate (2′,2′-difluorodeoxycytidine-5′-triphosphate; dFdCTP) without additional modifications of the tumor vasculature or stromal composition would be sufficient to improve therapeutic response in tumor-bearing KPC mice. Gemcitabine is either rapidly phosphorylated inside cells to the active compound dFdCTP or quickly enzymatically inactivated both inside and outside cells from its native form (2′,2′-difluorodeoxycytidine; dFdC) to the inactivate metabolite 2′,2′-difluorodeoxyuridine (dFdU) by the enzyme cytidine deaminase (CDA), and CDA is highly expressed in murine PDA neoplastic cells (29). First, we established the pharmacokinetic and pharmacodynamic profile of gemcitabine metabolites in KPC mice using a highly sensitive LC-MS/MS assay (30). Accordingly, plasma (Fig. S1*A*), tumor (Fig. S1 *B* and *C*), and intestine (Fig. S1*D*) tissue biopsies from KPC mice were obtained following i.p. treatment with gemcitabine. LC-MS/MS analysis was used to measure gemcitabine metabolites, and the immunohistochemical detection of phosphohistone H3 (PH3) and cleaved caspase 3 (CC3) was used to assess cellular proliferation and apoptosis, respectively. This analysis revealed that the peak of apoptotic cell death coincided with the peak of dFdCTP 2 h after gemcitabine administration (Fig. S1 *B–D*), and that decreases in proliferation were nearly complete at this time. Based upon these data, we chose to analyze all subsequent pharmacokinetic and pharmacodynamic parameters of gemcitabine 2 h after the last dose.

To investigate whether increasing chemotherapy concentrations alone is sufficient to elicit improved response rates, we used the CDA inhibitor 3,4,5,6-tetrahydrouridine (THU) (31, 32) to decrease the degradation and elimination of gemcitabine. Gemcitabine and THU were coadministered in tumor-bearing KPC mice, followed by the analysis of gemcitabine metabolites in plasma and PDA tumor biopsies. Inhibition of CDA by THU significantly increased dFdC and decreased dFdU concentrations in the plasma of mice (Fig. 1*A*). In tumor biopsies, the active, cytotoxic metabolite dFdCTP was significantly increased by addition of THU compared with single-agent gemcitabine (Fig. 1*B*). Despite 10-fold higher dFdC plasma concentrations and two to threefold higher concentrations of intratumoral dFdCTP, the mean content of apoptotic cells was not elevated (Fig. 1*C*). The increase in dFdCTP upon THU treatment was comparable to the results reported with PEGPH20 but cannot be directly compared with the IPI-926/gemcitabine data, as a less sensitive method of gemcitabine quantification was used (12, 16). In addition, although prolonged treatment was precluded by increased systemic toxicity, a randomized two-arm treatment study with gemcitabine or gemcitabine/THU did not show significant responses over a week as determined by tumor volume measurements using high-resolution ultrasound (Fig. 1*D*). Taken together, these results show that increasing the concentration of active gemcitabine alone does not elicit significant responses in murine PDA.

CTGF Is Highly Expressed in Cancer-Associated Fibroblasts and Tumor Cells in the KPC Model. As increased accumulation of gemcitabine alone did not yield a therapeutic benefit, we reasoned that previously observed antitumor effects with SHH inhibition and HA depletion could partly be attributed to the removal of various, yet unidentified, survival cues within the stromal compartment of murine pancreas tumors. Accordingly, we characterized the

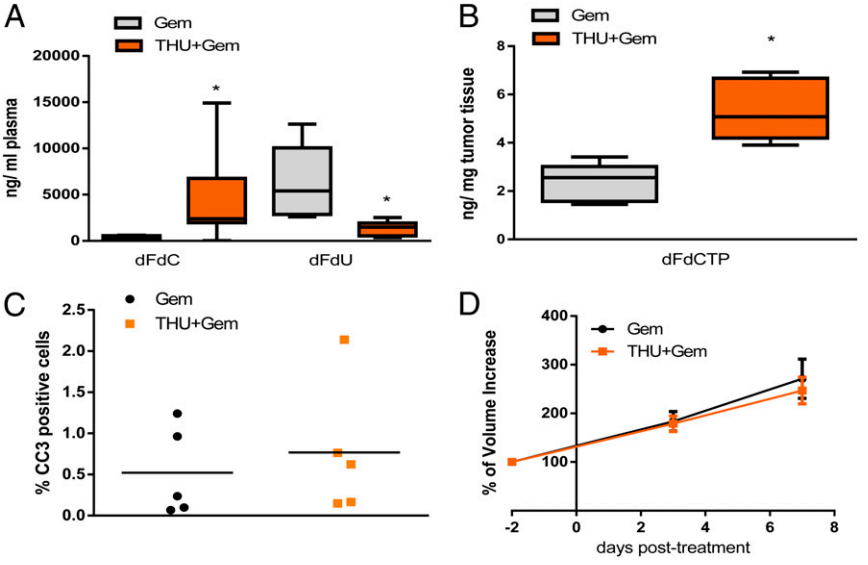

Fig. 1. Pharmacological inhibition of cytidine deaminase with THU increases intratumoral gemcitabine without altering tumor growth. (*A*) Plasma dFdU and dFdC concentrations in mice treated once with gemcitabine monotherapy ($n = 6$) or THU/gemcitabine combination ($n = 11$; $^*P < 0.005$). (*B*) Concentration of gemcitabine triphosphate (dFdCTP) in whole-tumor samples from KPC mice treated once with gemcitabine or THU/gemcitabine ($n = 5$ each cohort; $^*P < 0.05$). (*C*) Computer-based quantification of apoptosis (cleaved caspase 3) in individual tumors from mice treated once with gemcitabine or THU/gemcitabine (mean: 0.52 vs. 0.76; $n = 5$ each; $P = 0.6$). (*D*) Quantification of tumor volume growth using biweekly 3D high-resolution ultrasound in mice treated for 7 d with gemcitabine or THU/gemcitabine (mean 184.9% vs. 175.2%; $n = 7$ for both cohorts). All animals in *A–D* were killed 2 h after the last dose of gemcitabine.

function of CTGF in murine PDA because CTGF is expressed in human PDA and is known to participate in a large number of neoplastic cell–stromal interactions in cancers (23, 24). We found CTGF to be present in KPC tumor tissue with high expression in plasma and CAFs and lower but detectable levels in neoplastic cells (Fig. S2). Normal and metaplastic pancreata, as well as pancreatic intraepithelial neoplasia, exhibited no or very low CTGF content (Fig. S2*A*). Quantification of CTGF in tumor and plasma samples of KPC mice by ELISA showed a robust increase (about 50-fold) in CTGF protein compared with normal murine pancreas and plasma samples (Fig. S2 *B* and *C*). Western blot analysis revealed strong CTGF protein expression in α-smooth muscle actin (SMA)-positive and E-cadherin–negative CAFs, whereas primary KPC tumor cells showed very low CTGF protein (Fig. S2*D*). Because CTGF is overexpressed in tumor-bearing KPC mice in a similar pattern to what has been described in PDA patients (23, 24), this mouse model represents a tractable experimental platform to interrogate CTGF function in PDA.

CTGF Inhibition and Gemcitabine Reduce Tumor Burden and Induce Apoptosis in KPC Mice. FG-3019 is a therapeutic monoclonal human antibody against CTGF that is currently under clinical investigation in pancreatic cancer patients in a phase 1/2 study [national clinical trial (NCT)01181245]. To test the efficacy of CTGF inhibition in the KPC model, we treated mice with established tumors of comparable size for 9 d with normal human IgG, gemcitabine/IgG, FG-3019, or FG-3019/gemcitabine, and response to treatment was assessed by biweekly abdominal ultrasound examinations (Fig. 2*A* and Fig. S1 *E* and *F*). Consistent with clinical observations, gemcitabine/IgG treatment had only marginal effects on tumor growth. Final tumor volumes in mice treated with single-agent FG-3019 (mean: 244.7% growth, SE: 33.73) did not significantly differ from the gemcitabine/IgG cohort (193.5%, SE: 16.74; $P = 0.17$). Treatment with FG-3019/gemcitabine resulted in significantly smaller tumors (117.3%, SE: 10.91) compared with gemcitabine/IgG ($P < 0.02$) and IgG alone (236.7%, SE: 26.02; $P < 0.002$) (Fig. 2*A*). Tumor proliferation was assessed, and no significant differences were observed among the cohorts (Fig. 2*B*). In contrast, levels of intratumoral apoptosis were significantly and substantially elevated in the combination treatment compared with gemcitabine/IgG treatment (3-fold, $P < 0.005$), and less substantially but still significantly increased in FG-3019–treated versus IgG-treated tumors (1.8-fold, $P < 0.02$) (Fig. 2*C*). This increase in tumor cell apoptosis is consistent with the significantly reduced tumor burden after 9 d of treatment in FG-3019/gemcitabine–treated mice. Therefore, CTGF antagonism with FG-3019 and gemcitabine treatment synergize in murine PDA.

CTGF Inhibition Targets Epithelial Tumor Cells Without Increasing Intratumoral Gemcitabine Concentrations. As gemcitabine is known to elicit its antitumoral effects through induction of apoptosis, we sought to determine whether the enhanced antitumor activity of FG-3019/gemcitabine after 9 d of treatment stemmed in part from increased drug delivery caused by induction of apoptosis in fibroblasts and subsequent stromal collapse or stimulation of tumor angiogenesis. Accordingly, we performed a detailed histological analysis of tumors at the end point of the study (9 d) to assess potential alterations in the cellular and acellular composition of the tumor microenvironment. Interestingly, the number of α-SMA–positive fibroblasts and the amount and composition of collagen as determined by Picrosirius, Trichrome, and Herovici staining were unchanged (Fig. S3 *A*–*C*). Furthermore, fibronectin and secreted protein acidic and rich in cysteine (SPARC) were present in KPC mice (Fig. S3*A*) and unchanged by FG-3019 treatment. Also, the number of CD31-positive vessels did not significantly differ among the treatment cohorts

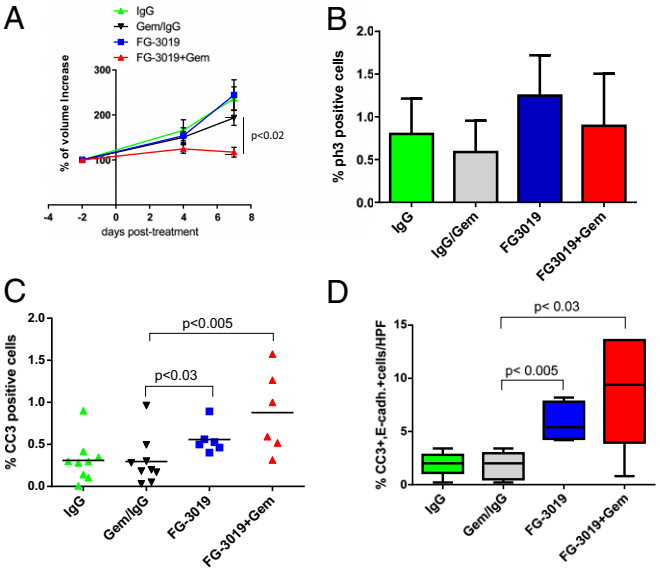

Fig. 2. FG-3019 targets CTGF to acutely decrease mouse PDA growth and induces neoplastic cell apoptosis. (*A*) Quantification of tumor volume growth over a 9-d treatment course with biweekly 3D high-resolution ultrasound shows a significant decrease in tumor burden in FG-3019/gemcitabine–treated mice ($n = 6$) compared with gemcitabine/IgG ($n = 10$; $P = 0.01$), IgG ($n = 9$; $P < 0.002$), and FG-3019 ($n = 6$; $P < 0.003$). (*B*) Computer-based quantification of proliferation (PH3) in tumors from corresponding mice treated with IgG, gemcitabine/IgG, FG-3019, and FG-3019/gemcitabine ($n \geq 5$ per cohort; error bars represent standard deviation). (*C*) Computer-based quantification of apoptosis (cleaved caspase 3) in tumors from corresponding mice treated with IgG, gemcitabine/IgG, FG-3019, and FG-3019/gemcitabine ($n \geq 6$ per cohort). (*D*) Quantification of E-cadherin/CC3–positive cells per high power field (HPF) reveals a significant increase in neoplastic cell apoptosis in FG-3019 ($P < 0.05$) and FG-3019/gemcitabine ($P < 0.03$) cohorts compared with gemcitabine/IgG and IgG ($n \geq 5$ per cohort). All animals were killed 2 h after the last dose of gemcitabine.

(Fig. S3*D*). Notably, coimmunofluorescence analyses revealed that the vast majority of apoptotic cells were E-cadherin–expressing neoplastic cells rather than α-SMA–expressing stromal cells, and these apoptotic cells were significantly increased in both FG-3019– and FG-3019/gemcitabine–treated mice (Fig. 2*D* and Fig. S3*E*).

We next examined the intratumoral levels of the gemcitabine prodrug dFdC as well as its inactivated and activated metabolites dFdU and dFdCTP, respectively. Interestingly, we found that concomitant treatment with FG-3019 and gemcitabine did not increase the levels of intratumoral gemcitabine metabolites (Fig. S3 *F*–*H*). Therefore, we conclude that the antitumor effect observed by antagonism of secreted CTGF in combination with gemcitabine is mediated by induction of apoptosis in neoplastic cells without increasing gemcitabine delivery or metabolism.

FG-3019 Decreases Expression of X-Linked Inhibitor of Apoptosis in PDA. We investigated candidate pathways previously demonstrated to augment pancreatic cancer cell survival, and found that the X-linked inhibitor of apoptosis (XIAP) protein level was markedly reduced in the lysates of FG-3019–treated KPC tumors (Fig. 3 *A* and *B*). This effect was most pronounced in FG-3019/gemcitabine combination-treated mice, consistent with the ability of *Xiap* silencing (33) or Xiap chemical inhibition (34) to sensitize PDA cell lines to additional therapies. *Xiap* mRNA levels were also significantly reduced by FG-3019 in the presence and absence of gemcitabine (Fig. 3*C*). To identify additional genes that could plausibly participate in the sensitization to PDA

CELL BIOLOGY

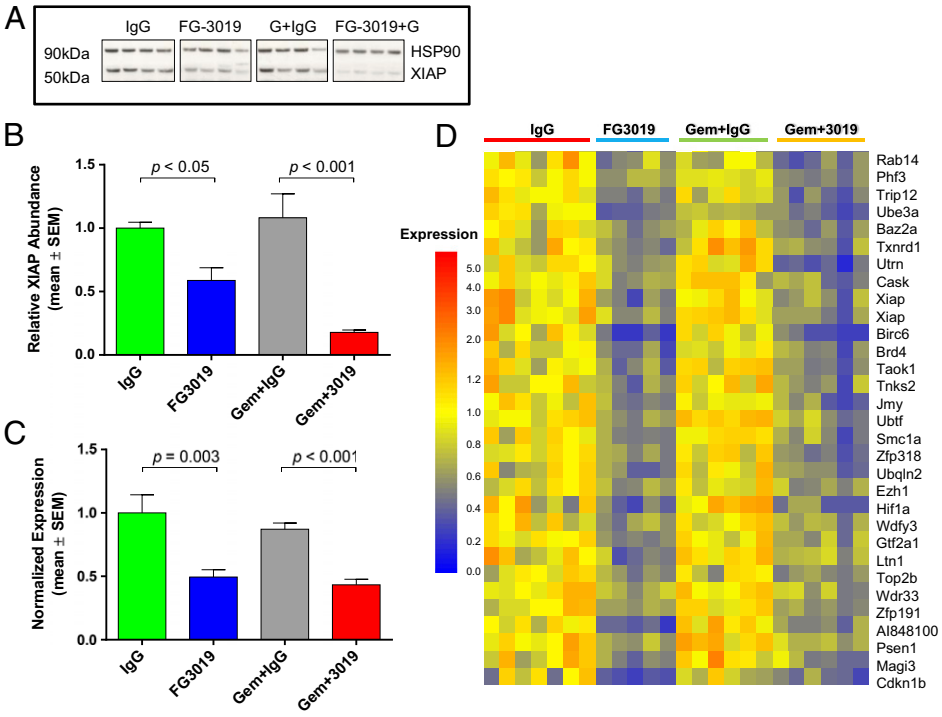

Fig. 3. FG-3019 decreases expression of XIAP in mouse PDA. (*A*) Western blot analysis of tumor lysates reveals decreased XIAP protein in FG-3019±gemcitabine cohorts following 9 d of treatment ($n = 4$ each). (*B*) Corresponding densitometry confirms significant decreases in HSP90-normalized XIAP protein levels in FG-3019 cohorts ($n = 4$ each; ANOVA with Newman–Keuls posttest). (*C*) *Xiap* regulation was confirmed by quantitative RT-PCR ($n \geq 5$ each cohort; ANOVA with Newman–Keuls posttest). (*D*) Bulk-tumor mRNA expression analysis followed by hierarchical clustering reveals 32 genes decreased (>1.5-fold, $P < 0.01$) by FG-3019 vs. IgG and FG-3019 + gemcitabine vs. IgG + gemcitabine for 9 d. XIAP protein levels in *B* correlated with mRNA expression data for corresponding tumors (microarrays, $r > 0.57$, $P < 0.05$).

cell death following FG-3019 treatment, we performed a whole-genome expression analysis using bulk-tumor mRNA. Surprisingly, only a small number of genes were coordinately down-regulated more than 1.5-fold ($P < 0.01$) by FG-3019 and FG-3019/gemcitabine compared with their respective control cohorts (Fig. 3*D*). Importantly, our analysis confirmed decreased expression of *Xiap* (two separate probes), and also identified the down-regulation of additional prosurvival transcripts such as *Birc6*, *Psen1*, *Ubqln2*, and *Hif1α* (Fig. 3*D*). Therefore, the reduced expression of Xiap and several additional genes correlates with FG-3019 and treatment response in murine PDA.

CTGF Inhibition in Combination with Gemcitabine Prolongs Survival and Reduces Hemorrhagic Ascites and Liver Metastasis in KPC Mice. To evaluate the effects of FG-3019 on intratumoral CTGF, we analyzed tumor lysates obtained after 9 d of treatment by immunoblotting. Full-length CTGF (37 kDa) could be detected in bulk-tumor lysates from treated and untreated KPC mice. Additionally, a 15- to 20-kDa protein fragment recognized by the CTGF antibody occurred exclusively in FG-3019– and FG-3019/gemcitabine–treated tumors (Fig. 4*A*). This fragment represents an amino-terminal cleaved CTGF fragment of uncertain function (35, 36) that is derived from the 37-kDa full-length CTGF protein, and its presence may indicate the intratumoral binding of CTGF by FG-3019 with exposure to extracellular proteases. Because the prior short-term experiments with FG-3019 indicated evidence of antineoplastic effects in PDA, we performed a randomized treatment study to determine whether these effects would translate to a survival advantage. Tumor-bearing KPC mice were enrolled with comparable tumor volumes (Fig. S4*A*), and tumor growth was monitored once per week by 3D ultrasonography. KPC mice treated with FG-3019 alone showed no survival benefit in comparison with gemcitabine-treated controls (11 versus 8 d). In contrast, combination treatment with FG-3019/gemcitabine extended the median survival of KPC mice to 29 d (Fig. 4*B*; $P = 0.03$, log-rank test). The majority of FG-3019/gemcitabine–treated KPC mice demonstrated objective slowing of tumor growth without evidence of obvious tumor shrinkage. In addition, FG-3019/gemcitabine treatment resulted in a significant decrease of hemorrhagic ascites (4/10) compared with gemcitabine alone (13/16) at end point (Fig. 4*C*; $P < 0.05$). Histopathological evaluation revealed no clear differences in tumor morphology, extracellular matrix composition, or vascular density following FG-3019/gemcitabine treatment. In particular, collagen I+III content as determined by polarized light microscopy of Picrosirius red stains did not show significant differences (Fig. S4*B*). Interestingly, the number and size of metastases throughout the liver were reduced in FG-3019/gemcitabine–treated KPC mice, albeit not in a statistically significant manner compared with gemcitabine monotherapy (Fig. S4*C*).

Discussion

As conventional and targeted treatment approaches have largely failed to achieve substantial treatment responses in pancreatic cancer patients, novel therapies are urgently needed in the clinic. The notion that the pronounced desmoplastic reaction in PDA actively contributes to the unusual refractoriness of PDA to systemic therapies has stimulated this area of research and revealed candidate therapeutic targets. Nonetheless, a potential role for desmoplasia in drug resistance has been only partially addressed, due to the multitude of signaling interactions between tumor cells and the surrounding microenvironment (37–40).

We and others have previously shown that depletion of abundant ECM components improves perfusion of hypovascular

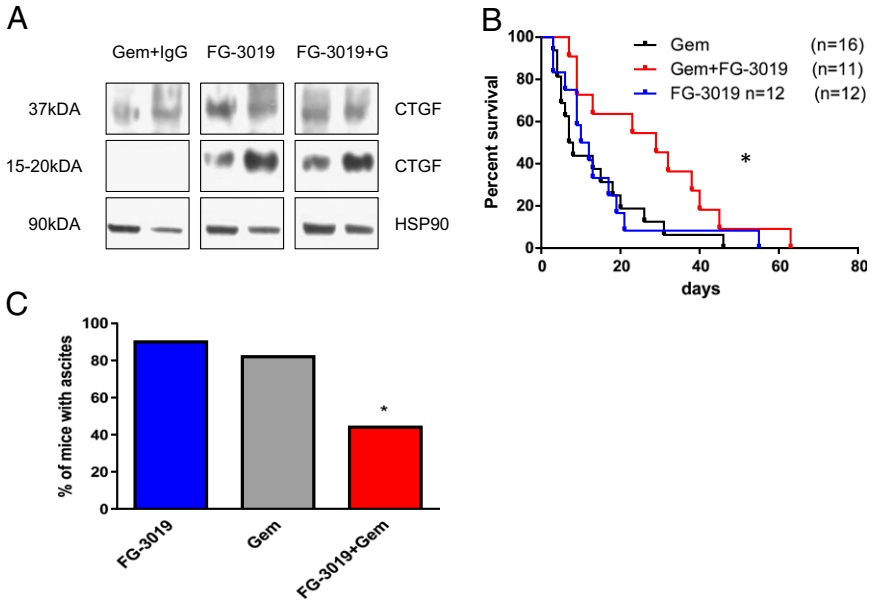

Fig. 4. FG-3019 targets CTGF to prolong survival when combined with gemcitabine in the KPC mouse model. (*A*) Western blot analysis of whole-tumor lysates from KPC mice treated for 9 d showing a cleaved CTGF fragment (15–20 kDa) in an FG-3019–treated specimen. (*B*) Survival is extended by the combination of FG-3019/gemcitabine (median survival, gemcitabine 7.5 d vs. 29 d with FG-3019/gemcitabine, $*P = 0.03$; FG-3019 monotherapy, 11 d). (*C*) Malignant hemorrhagic ascites was significantly decreased at end point in KPC mice treated with the combination of FG-3019/gemcitabine ($n = 10$; $*P < 0.04$, Fisher's exact test) compared with gemcitabine ($n = 16$) and FG-3019 ($n = 9$).

pancreas tumors, allowing the accumulation of higher intratumoral drug concentrations (12, 15, 16). However, these studies could not address whether increased drug delivery itself or the combination of stromal modulation and chemotherapy was deterministic regarding the improved responses to treatment. Here we uncouple drug delivery from stromal disruption to show that increased intratumoral concentrations of gemcitabine are alone insufficient to overcome therapeutic resistance in murine PDA. Furthermore, we identify CTGF as an important factor in the tumor microenvironment of the KPC model mediating therapeutic resistance. Although CTGF antagonism would be hypothesized to disrupt the fibrotic architecture of PDA tumors, we instead found that FG-3019 treatment left the stromal content grossly intact. Also, in contrast to previous xenograft results with FG-3019 that demonstrated antitumor activity (41, 42), treatment with FG-3019 alone did not result in significant antitumoral responses in KPC mice. Previous reports have also described CTGF as a critical mediator of vascular remodeling by regulating pericyte function and endothelial basement membrane formation during angiogenesis (43). In the tumor microenvironment, CTGF and the CXCR2 chemokine ligand axis have also been implicated as promoters of tumor angiogenesis in a variety of PDA models (42, 44). In contrast to the prior finding that inhibition of CXCR2 resulted in reduced CTGF levels and regulated blood vessel density and tumor growth in the related $Ptf1a^{cre/+};LSL\text{-}Kras^{G12D/+};Tgfbr2^{flox/flox}$ mouse model (44), FG-3019 had no effect on mean vessel density over the time course of treatment in KPC mice, and suggests that the relevant therapeutic targets here are neoplastic cell-intrinsic.

CTGF antagonism with FG-3019 required the combined treatment with gemcitabine to promote tumor stabilization and prolong survival, indicating that CTGF provides survival cues to PDA cells that counteract the cytotoxic response to gemcitabine. Indeed, candidate-based and genome-wide approaches implicated XIAP as one potential mediator of PDA cell survival downstream of CTGF function. XIAP belongs to the family of inhibitor of apoptosis proteins that can directly inhibit caspases 3, 7, and 9 (45), and the strong inverse link between chemotherapy responsiveness and XIAP expression in several cancers (33, 46–48) may extend our finding of a unique CTGF–XIAP axis in murine pancreas cancer to other tumor types. The molecular details of transcriptional and posttranscriptional *Xiap* regulation by CTGF in PDA may provide additional means to increase the antineoplastic effects of FG-3019. Furthermore, several other prosurvival genes such as *Birc6*, *Psen1*, *Ubqln2*, and *Hif1α* were down-regulated in response to FG-3019, and could conceivably also play a role in chemosensitivity in PDA.

The identified mechanism of increased response following combined treatment with FG-3019 and gemcitabine is distinct from increased gemcitabine delivery, and may also involve other pathways known to be regulated by CTGF including stromal cell-secreted paracrine ligands and neoplastic–stromal interactions. Interestingly, Straussman and colleagues recently reported that primary human diploid fibroblasts suppressed the response of PDA cell lines to gemcitabine when cocultured in vitro, but did not identify the pathways responsible for this finding (40). This report is consistent with our own work, where we identify CTGF as a candidate that modulates PDA neoplastic cell responses to gemcitabine via regulation of prosurvival pathways including XIAP.

These results and our prior work (17) suggest that disrupting the stromal barrier to increase drug delivery is not required to increase antitumor responses in murine PDA models. Rather, increased drug delivery may be most relevant when various intratumoral survival cues are concomitantly disrupted. We propose here that CTGF represents one such regulator of neoplastic survival cues during gemcitabine treatment, and our results are particularly germane given the ongoing investigational trial with this therapeutic combination (NCT01181245). In a wider sense, our study adds to the growing body of evidence that tumor–stromal interactions critically contribute to innate drug resistance observed in pancreatic cancer and other malignancies.

Materials and Methods

Additional details are provided in *SI Materials and Methods*.

Western Blot Analysis. Western blots were performed as previously described (49). Densitometry was performed by scanning films on an ImageScanner

III (GE Healthcare). Images were processed using LabScan 6.0 and ImageQuant TL 9.0 software (GE Healthcare) to quantify signal and normalize to Hsp90.

Quantitative PCR. Quantitative real-time PCR was performed on a 7900HT Real-Time PCR System using relative quantification (ΔΔCt) with TaqMan assays Mm00776505_m1 and 4352341E (Applied Biosystems).

mRNA Expression Profiling. Tumor mRNA profiling was performed using Affymetrix mouse genome 430A 2.0 arrays (Gene Expression Omnibus accession no. GSE46203). GeneChip Robust Multiarray Averaging (GC-RMA) processed, median normalized data were analyzed using Agilent GeneSpring GX software.

Statistical Analysis. Statistical analysis was carried out using GraphPad Prism version 5.01 (GraphPad Software). The log-rank test was performed on the Kaplan–Meier survival curves, and the Mann–Whitney nonparametric *U* test was used for all other analyses if not indicated otherwise. Results are presented as mean ± standard error of mean (SEM) if not indicated otherwise. $P < 0.05$ was considered to be significant.

ACKNOWLEDGMENTS. We thank Mona Spector and Daniel Olund for critical comments on the manuscript; and Frances Connor, Paul Mackin, and Lisa Young for maintenance and management of mouse colonies, as well as staff from the Cambridge Research Institute Biological Resource Unit, histology core, and pharmacokinetics core. This research was supported by the University of Cambridge and Cancer Research UK, The Li Ka Shing Foundation and Hutchison Whampoa Limited, and the National Institute for Health Research Cambridge Biomedical Research Centre. D.A.T. is also supported by the Lustgarten Foundation for Pancreatic Cancer Research and by the Cold Spring Harbor Laboratory Association. K.K.F. and D.A.T. were supported by European Community Grant EPC-TM-Net 256974. A.N. was supported by a Deutsche Krebshilfe Mildred Scheel postdoctoral fellowship and by a research grant of the University Medical Center Giessen and Marburg. D.I.J. is a Group Leader in the Cancer Research UK Cambridge Research Institute. T.E.B. is supported by Cancer Research UK.

1. Siegel R, Naishadham D, Jemal A (2012) Cancer statistics, 2012. *CA Cancer J Clin* 62(1): 10–29.
2. Burris HA III, et al. (1997) Improvements in survival and clinical benefit with gemcitabine as first-line therapy for patients with advanced pancreas cancer: A randomized trial. *J Clin Oncol* 15(6):2403–2413.
3. Conroy T, et al.; Groupe Tumeurs Digestives of Unicancer; PRODIGE Intergroup (2011) FOLFIRINOX versus gemcitabine for metastatic pancreatic cancer. *N Engl J Med* 364 (19):1817–1825.
4. Beatty GL, et al. (2011) CD40 agonists alter tumor stroma and show efficacy against pancreatic carcinoma in mice and humans. *Science* 331(6024):1612–1616.
5. Clark CE, et al. (2007) Dynamics of the immune reaction to pancreatic cancer from inception to invasion. *Cancer Res* 67(19):9518–9527.
6. Bayne LJ, et al. (2012) Tumor-derived granulocyte-macrophage colony-stimulating factor regulates myeloid inflammation and T cell immunity in pancreatic cancer. *Cancer Cell* 21(6):822–835.
7. Rhim AD, et al. (2012) EMT and dissemination precede pancreatic tumor formation. *Cell* 148(1-2):349–361.
8. Cook N, Jodrell DI, Tuveson DA (2012) Predictive in vivo animal models and translation to clinical trials. *Drug Discov Today* 17(5-6):253–260.
9. Gopinathan A, Tuveson DA (2008) The use of GEM models for experimental cancer therapeutics. *Dis Model Mech* 1(2-3):83–86.
10. Olson P, Chu GC, Perry SR, Nolan-Stevaux O, Hanahan D (2011) Imaging guided trials of the angiogenesis inhibitor sunitinib in mouse models predict efficacy in pancreatic neuroendocrine but not ductal carcinoma. *Proc Natl Acad Sci USA* 108(49): E1275–E1284.
11. Hingorani SR, et al. (2005) Trp53R172H and KrasG12D cooperate to promote chromosomal instability and widely metastatic pancreatic ductal adenocarcinoma in mice. *Cancer Cell* 7(5):469–483.
12. Olive KP, et al. (2009) Inhibition of Hedgehog signaling enhances delivery of chemotherapy in a mouse model of pancreatic cancer. *Science* 324(5933):1457–1461.
13. Thompson CB, et al. (2010) Enzymatic depletion of tumor hyaluronan induces antitumor responses in preclinical animal models. *Mol Cancer Ther* 9(11):3052–3064.
14. Jiang P, et al. (2012) Effective targeting of the tumor microenvironment for cancer therapy. *Anticancer Res* 32(4):1203–1212.
15. Provenzano PP, et al. (2012) Enzymatic targeting of the stroma ablates physical barriers to treatment of pancreatic ductal adenocarcinoma. *Cancer Cell* 21(3): 418–429.
16. Jacobetz MA, et al. (2013) Hyaluronan impairs vascular function and drug delivery in a mouse model of pancreatic cancer. *Gut* 62(1):112–120.
17. Cook N, et al. (2012) Gamma secretase inhibition promotes hypoxic necrosis in mouse pancreatic ductal adenocarcinoma. *J Exp Med* 209(3):437–444.
18. Xie D, et al. (2001) Breast cancer. Cyr61 is overexpressed, estrogen-inducible, and associated with more advanced disease. *J Biol Chem* 276(17):14187–14194.
19. Xie D, Nakachi K, Wang H, Elashoff R, Koeffler HP (2001) Elevated levels of connective tissue growth factor, WISP-1, and CYR61 in primary breast cancers associated with more advanced features. *Cancer Res* 61(24):8917–8923.
20. Pan LH, et al. (2002) Neoplastic cells and proliferating endothelial cells express connective tissue growth factor (CTGF) in glioblastoma. *Neurol Res* 24(7):677–683.
21. Koliopanos A, et al. (2002) Connective tissue growth factor gene expression alters tumor progression in esophageal cancer. *World J Surg* 26(4):420–427.
22. Zeng ZJ, Yang LY, Ding X, Wang W (2004) Expressions of cysteine-rich61, connective tissue growth factor and Nov genes in hepatocellular carcinoma and their clinical significance. *World J Gastroenterol* 10(23):3414–3418.
23. Wenger C, et al. (1999) Expression and differential regulation of connective tissue growth factor in pancreatic cancer cells. *Oncogene* 18(4):1073–1080.
24. Hartel M, et al. (2004) Desmoplastic reaction influences pancreatic cancer growth behavior. *World J Surg* 28(8):818–825.
25. Iacobuzio-Donahue CA, Ryu B, Hruban RH, Kern SE (2002) Exploring the host desmoplastic response to pancreatic carcinoma: Gene expression of stromal and neoplastic cells at the site of primary invasion. *Am J Pathol* 160(1):91–99.
26. Bennewith KL, et al. (2009) The role of tumor cell-derived connective tissue growth factor (CTGF/CCN2) in pancreatic tumor growth. *Cancer Res* 69(3):775–784.
27. Gao R, Brigstock DR (2006) A novel integrin alpha5beta1 binding domain in module 4 of connective tissue growth factor (CCN2/CTGF) promotes adhesion and migration of activated pancreatic stellate cells. *Gut* 55(6):856–862.
28. Gao R, Brigstock DR (2005) Connective tissue growth factor (CCN2) in rat pancreatic stellate cell function: Integrin alpha5beta1 as a novel CCN2 receptor. *Gastroenterology* 129(3):1019–1030.
29. Frese KK, et al. (2012) nab-paclitaxel potentiates gemcitabine activity by reducing cytidine deaminase levels in a mouse model of pancreatic cancer. *Cancer Discov* 2(3): 260–269.
30. Bapiro TE, et al. (2011) A novel method for quantification of gemcitabine and its metabolites 2′,2′-difluorodeoxyuridine and gemcitabine triphosphate in tumour tissue by LC-MS/MS: Comparison with (19)F NMR spectroscopy. *Cancer Chemother Pharmacol* 68(5):1243–1253.
31. Beumer JH, et al. (2008) Plasma pharmacokinetics and oral bioavailability of 3,4,5,6-tetrahydrouridine, a cytidine deaminase inhibitor, in mice. *Cancer Chemother Pharmacol* 62(3):457–464.
32. Beumer JH, et al. (2008) Modulation of gemcitabine (2′,2′-difluoro-2′-deoxycytidine) pharmacokinetics, metabolism, and bioavailability in mice by 3,4,5,6-tetrahydrouridine. *Clin Cancer Res* 14(11):3529–3535.
33. Shrikhande SV, et al. (2006) Silencing of X-linked inhibitor of apoptosis (XIAP) decreases gemcitabine resistance of pancreatic cancer cells. *Anticancer Res* 26(5A):3265–3273.
34. Karikari CA, et al. (2007) Targeting the apoptotic machinery in pancreatic cancers using small-molecule antagonists of the X-linked inhibitor of apoptosis protein. *Mol Cancer Ther* 6(3):957–966.
35. Brigstock DR, et al. (1997) Purification and characterization of novel heparin-binding growth factors in uterine secretory fluids. Identification as heparin-regulated Mr 10,000 forms of connective tissue growth factor. *J Biol Chem* 272(32):20275–20282.
36. Ball DK, et al. (1998) Characterization of 16- to 20-kilodalton (kDa) connective tissue growth factors (CTGFs) and demonstration of proteolytic activity for 38-kDa CTGF in pig uterine luminal flushings. *Biol Reprod* 59(4):828–835.
37. Neesse A, et al. (2011) Stromal biology and therapy in pancreatic cancer. *Gut* 60(6): 861–868.
38. Hanahan D, Weinberg RA (2011) Hallmarks of cancer: The next generation. *Cell* 144(5):646–674.
39. Wang W, et al. (2009) Crosstalk to stromal fibroblasts induces resistance of lung cancer to epidermal growth factor receptor tyrosine kinase inhibitors. *Clin Cancer Res* 15(21):6630–6638.
40. Straussman R, et al. (2012) Tumour micro-environment elicits innate resistance to RAF inhibitors through HGF secretion. *Nature* 487(7408):500–504.
41. Dornhöfer N, et al. (2006) Connective tissue growth factor-specific monoclonal antibody therapy inhibits pancreatic tumor growth and metastasis. *Cancer Res* 66(11): 5816–5827.
42. Aikawa T, Gunn J, Spong SM, Klaus SJ, Korc M (2006) Connective tissue growth factor-specific antibody attenuates tumor growth, metastasis, and angiogenesis in an orthotopic mouse model of pancreatic cancer. *Mol Cancer Ther* 5(5):1108–1116.
43. Hall-Glenn F, et al. (2012) CCN2/connective tissue growth factor is essential for pericyte adhesion and endothelial basement membrane formation during angiogenesis. *PLoS One* 7(2):e30562.
44. Ijichi H, et al. (2011) Inhibiting Cxcr2 disrupts tumor-stromal interactions and improves survival in a mouse model of pancreatic ductal adenocarcinoma. *J Clin Invest* 121(10): 4106–4117.
45. Deveraux QL, Takahashi R, Salvesen GS, Reed JC (1997) X-linked IAP is a direct inhibitor of cell-death proteases. *Nature* 388(6639):300–304.
46. Schimmer AD, et al. (2004) Small-molecule antagonists of apoptosis suppressor XIAP exhibit broad antitumor activity. *Cancer Cell* 5(1):25–35.
47. Lopes RB, Gangeswaran R, McNeish IA, Wang Y, Lemoine NR (2007) Expression of the IAP protein family is dysregulated in pancreatic cancer cells and is important for resistance to chemotherapy. *Int J Cancer* 120(11):2344–2352.
48. Vogler M, et al. (2008) Targeting XIAP bypasses Bcl-2-mediated resistance to TRAIL and cooperates with TRAIL to suppress pancreatic cancer growth in vitro and in vivo. *Cancer Res* 68(19):7956–7965.
49. Karreth FA, DeNicola GM, Winter SP, Tuveson DA (2009) C-Raf inhibits MAPK activation and transformation by B-Raf(V600E). *Mol Cell* 36(3):477–486.